Early Increases in Breast Tumor Xenograft Water Mobility in Response to Paclitaxel Therapy Detected by Non-Invasive Diffusion Magnetic Resonance Imaging

Jean-Philippe Galons[*], *Maria I. Altbach*[*], *Gillian D. Paine-Murrieta*[†], *Charles W. Taylor*[†] *and Robert J. Gillies*[*†]

[*] Department of Radiology, [†]Arizona Cancer Center, University of Arizona, Tucson, AZ

Abstract

An important goal in cancer chemotherapy is to sensitively and quantitatively monitor the response of individual patients' tumors to successful, or unsuccessful, therapy so that regimens can be altered iteratively. Currently, tumor response is monitored by frank changes in tumor morphology, yet these markers take long to manifest and are not quantitative. Recent studies suggest that the apparent diffusion coefficient of water (ADC_w), measured noninvasively with magnetic resonance imaging, is sensitively and reliably increased in response to successful CTx. In the present study, we investigate the combination chemotherapy response of human breast cancer tumor xenografts sensitive or resistant to Paclitaxel by monitoring changes in the ADC_w. Our results indicate that there is a clear, substantial, and early increase in the ADC_w after successful therapy in drug sensitive tumors and that there is no change in the ADC_w in p-glycoprotein–positive tumors, which are resistant to Paclitaxel. The mechanism underlying these changes is unknown yet is consistent with apoptotic cell shrinkage and a concomitant increase in the extracellular water fraction.

Introduction

Breast cancer is the second leading cause of death, after lung cancer, in American women. Paclitaxel, an inhibitor of microtubule depolymerization, is an effective chemotherapeutic agent in the adjuvant treatment of breast cancer, with a response rate ranging from 32% to 56% alone, or from 44% to 100% in combination chemotherapy (CTx) with anthracyclines [1]. An important goal in cancer CTx is to tailor treatment regimens to individual patients' genotype, tumor type, and physiology. In order to accomplish this, it will be essential to sensitively and quantitatively monitor the response of individual patients' tumors to successful, or unsuccessful, therapy so that regimens can be altered adaptively. Currently, tumor response is monitored by frank changes in tumor morphology, such as the size or margins of the tumor. However, these macroscopic markers take long to manifest and typically are not quantitative or quantified with modest precision. An intriguing potential improvement in therapeutic monitoring is the noninvasive measurement of the apparent diffusion coefficient of water (ADC_w) by magnetic resonance imaging (MRI). Recent studies have shown that diffusion-weighted MRI (DWI) can detect tumor response to CTx sensitively, quantitatively, and early [2–5]. In the present study, we investigate the CTx response of drug-sensitive and drug-resistant human tumor xenografts to Paclitaxel by monitoring changes in the ADC_w by DWI.

Paclitaxel is a microtubule depolymerization inhibitor commonly used in CTx. It was chosen because it is an extremely potent drug against tumors from MCF7/S cells. Its clinical antitumor activity has been demonstrated in patients with malignancies such as carcinoma of the ovaries, breast, lung, bladder, testes, esophagus, and endometrium [6]. It has also been shown to be more modestly active against Kaposi's sarcoma, lymphoma, and carcinoma of the cervix and stomach [6]. In contrast, taxanes do not have significant activity against neoplasms derived from tissues that overexpress p-glycoprotein (P-gp), including human breast tumor cells [7,8].

DWI is an early, noninvasive indicator of ischemic insult and can be used to successfully diagnose the extent of injury and the response to therapy in a variety of nontumor systems such as brain [9–11]. To date, it has been used primarily in neurological MRI examinations. The physiological mechanisms underlining the ADC_w changes in these systems are thought to involve a shift of water between extracellular and intracellular compartments that accompanies cell swelling or shrinkage. Recently published models have provided a theoretical framework wherein ischemic-associated changes in ADC_w can be interpreted [12,13]. In the case of stroke, decreases in ADC_w values are consistent with cell swelling, causing a shift of water from the extracellular to the intracellular space [14,15]. In the case of rapid hemodialysis of nephrectomized rats, the observed increases of ADC_w are consistent with hypernatremia-induced cell shrinkage and concomitant accumulation of water in the extracellular space [16]. The measurement of ADC_w has not been extensively applied to the study of cancer CTx. However, in the few extant studies, the results are extremely promising.

The use of DWI to monitor the response of tumors to CTx was first proposed by Ross and Chenevert [2,17]. Subsequently, Evelhoch's group [4,5] used ^1H MRS to measure the ADC_w in sarcoma xenografts to detect an early re-

Address correspondence to: Jean-Philippe Galons, Dept. Radiology, Arizona Health Sciences Center, Tucson, AZ 85724. E-mail: jgalons@u.arizona.edu
Received 31 December 1998; Accepted 22 January 1999.

sponse to cyclophosphamide (Cp) and 5-fluorouracil (5FU). In the case of Cp, ADC_w was measured before commencement of CTx and up to 9 days after treatment. Tumor ADC_w increased significantly within 2 days of treatment, which was prior to any observable change in tumor volume or other MRI visible changes. Results with 5FU were similar. Cp is a DNA alkylating agent and 5FU is an antimetabolite. In the present study, we use Paclitaxel, which acts via a distinct mechanism, to test the hypothesis that changes in ADC_w are a general response to successful CTx. In addition, our study measured the ADC_w by DWI, as compared to whole-tumor measurements. The advantage of using DWI is that spatial distribution of the ADC_w in the tumor is obtained. Thus, the responsiveness of various parts in the tumor to CTx can be analyzed.

Materials and Methods

Cell Lines and Tumors

In the current study Paclitaxel (MeadJohnson, Princeton, NJ) was used as CTx agent against tumors grown in severe combined immunodeficient (SCID) mice from MCF7/S and MCF7/D40 cell lines. MCF7/S cells are parental, drug sensitive, breast carcinoma cells that were originally obtained from American Type Culture Collection (ATCC #HTB-22, Rockville, MD). MCF7/D40 were generated *in vitro* by successive culturing in increasing concentrations of doxorubicin. These cells are (P-gp) positive and are 40-fold resistant to doxorubicin, compared to MCF7/S. The CTx responses of these cells to a variety of drugs have been demonstrated *in vitro* and *in vivo* [18].

SCID mice were obtained from the SCID mouse core facility at the University of Arizona Comprehensive Cancer Center. Tumors were grown by implanting 5×10^6 cells in Matrigel (Collaborative Research, Bedford, MA) into the mouse flanks. After 4 to 5 days, tumors reached a size (200–400 mm^3) appropriate for MRI analyses. Paclitaxel-treated animals were injected intraperitoneally with a single dose (27 mg/kg) immediately after the first MRI experiment and given subsequent booster injections (18 mg/kg) every other day. Control mice were injected an equivalent volume of a 0.9% saline solution.

SCID mice are a good system with which to examine the effects of chemotherapeutic agents on human tumor xenografts [19]. Melanoma, colon carcinoma, lung carcinoma, leukemia, prostate, and breast cell lines have all been successfully grown to tumors in SCID mice and successfully treated with CTx, e.g., tamoxifen (breast); Paclitaxel (breast); Cp (breast, leukemia); carmustine (colon), cisplatin (colon); and doxorubicin (leukemia). Therapeutic responses have been determined from tumor volumes, measured with calipers and calculated according to the formula (length $\times$ width^2)/2 [20].

Measurement of ADC_w

MRI was done on a 40 cm clear bore Bruker Biospec 4.7 Tesla (200 MHz ^{1}H) imaging spectrometer (Bruker, Karlsruhe, Germany). In all cases, animals were anesthetized with ketamine:acepromazine:xylazine at 72:6:6 mg/kg, and tumors were placed within a 1 cm diameter, 2-turn solenoidal coil. In DWI, the sample is pulsed with a strong magnetic field gradient, which imparts spatially dependent phase shifts on individual spins (e.g., water protons). After an evolution time, a refocusing pulse is imposed such that stationary spins (i.e., those with low diffusion coefficient, ADC_w) will completely refocus, whereas spins that have moved during the evolution time (i.e., those with high ADC_w) will not refocus, leading to signal attenuation. In DWI, the magnitude of signal is reduced by increasing the gradient strength or the evolution time Eq. (1). The parameters of gradient strength and evolution time are combined in the *b-factor*. DWI were obtained by using a diffusion-weighted stimulated echo pulse sequence [21] at 3 different *b* values. Other imaging parameters included TE, 10 ms; TR, 500 ms; diffusion time Δ, 50 ms; diffusion-weighting gradients duration δ, 4 ms; FOV 2.5 cm, matrix size 128×128).

DWI were then fit on a pixel-by-pixel basis to Eq. (1) by using a routine written for this purpose in interactive data language (IDL). Eq. (1) relates the decrease in signal intensity observed with increasing *b-factor* or ADC_w:

$$S = S_0 e^{-b(\mathrm{ADC})} \tag{1}$$

with

$$b = \gamma^2 G^2 \delta^2 (\Delta - \delta/3)$$

where S and S_0 are the signal intensities in each pixel with and without diffusion weighting, respectively; δ is the diffusion-weighting pulse duration; Δ the delay between the start of the diffusion-weighting pulse; γ the gyromagnetic ratio; and *G* the gradient strength. In the calculation of *b* values, cross terms between diffusion-weighting gradients and imaging gradients were taken into account. A possible source of error is the potential anisotropic nature of tumor tissue. In the presence of anisotropy the measured ADC_w

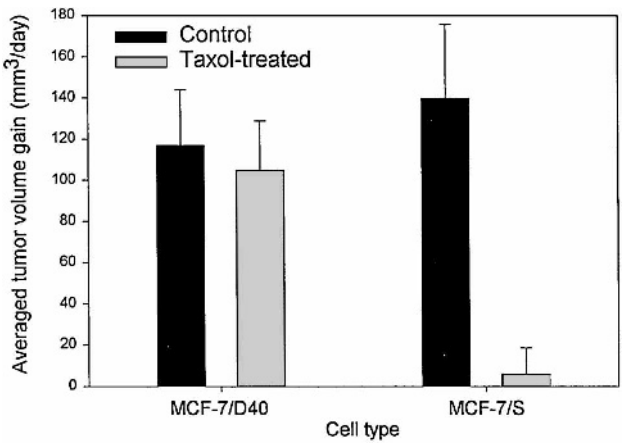

Figure 1. *Tumor volume–based response indexes to Paclitaxel for MCF7/S and MCF7/D40 tumors. In these experiments, the response indexes for the MCF7/D40 and MCF7/S tumors were calculated over a 7-day treatment regime.*

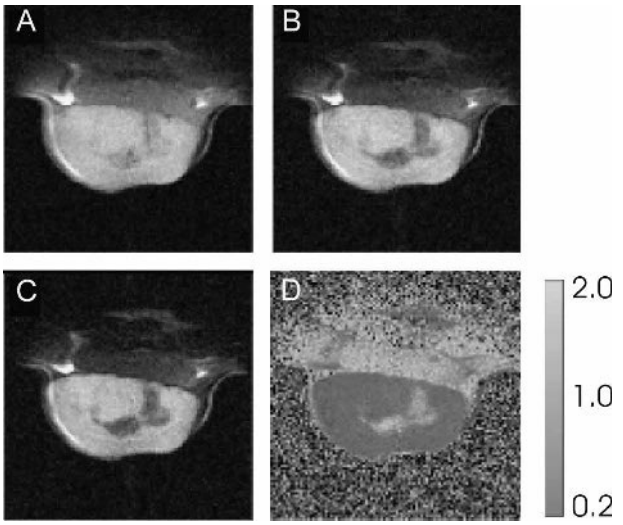

Figure 2. *DWI obtained from a 12-day-old tumor at different values of the diffusion-weighting factor, b. A. $b = 0.027 \times 10^9$ s/m^2, B. $b = 0.249 \times 10^9$ s/m^2, C. $b = 0.442 \times 10^9$ s/m^2. D. ADC_w map calculated from the images shown in A through C. Final ADC_w values were obtained by summing 3 ADC_w maps obtained with diffusion weighting in 3 orthogonal directions (see Materials and Methods).*

becomes a function of the orientation of the tumor relative to the direction of the diffusion gradients. To overcome this problem, we measured ADCs in 3 orthogonal directions and calculated the trace of the ADC_w, a parameter independent of orientation [22].

Results

Response of MCF-7 Tumors to Paclitaxel in Vivo

Figure 1 shows the responses of 8 MCF7/S and 8 MCF7/D40 tumors after treatment with Paclitaxel. Although tumor growth was exponential, data were expressed as the increase in tumor volumes by day 7, normalized to an average per-day basis. As shown in this figure, untreated tumors increase in volume at a rate of 115 to 140 mm^3 per day. In response to Paclitaxel, the drug-sensitive MCF7/S tumors uniformly halted tumor growth, with average volume gains near 5 mm^3 per day, whereas the drug-resistant tumors continued to grow, with volume gains greater than 105 mm^3 per day. The growth rate of the drug-resistant tumors was indistinguishable from the growth rate of untreated tumors. These data demonstrate that the SCID mouse model is relevant to study the response of Paclitaxel CTx in drug-sensitive and drug-resistant tumors grown from MCF7/S and MCF7/D40 cell lines, respectively.

Measurements of ADC_w in MCF7 Tumors

DWI images at different *b*-factors are shown in Figure 2A to C from a representative MCF7 tumor implanted in the

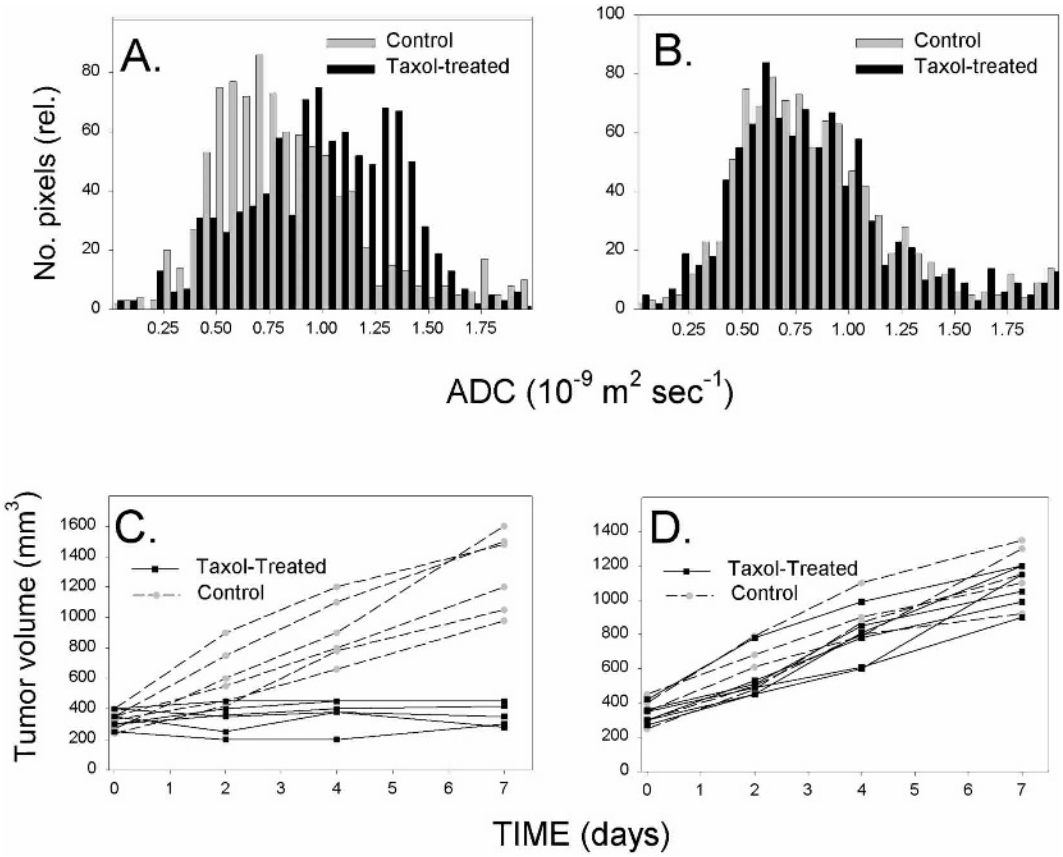

Figure 3. *(A,B) Effect of Paclitaxel on the distribution of ADC_w values in MCF7/S and MCF7/D40 tumors compared to untreated tumors. ADCw values were obtained 48 hours after the beginning of CTx. To allow for a direct comparison, the number of pixels in each tumor was normalized to a value of 1000 and the data averaged for each group (treated and control mice). (C,D) Effect of Paclitaxel on the growth of MCF7/S and MCF7/D40 tumors compared to untreated tumors.*

flanks of a SCID mouse. Note that the image shown was obtained 12 days after tumor inoculation to illustrate the diffusion behavior of necrosis. As the *b*-factor is increased, the pixel intensities inversely reflect the diffusion of the water molecules in the tumor (i.e., the higher the diffusion, the more rapidly the signal intensity is attenuated). Thus, signals originating from the necrotic spaces (dark regions within the tumor) lose intensity faster than the surrounding viable regions of the tumor. This is due to a higher diffusion of water in these regions of the tumor with lower cellularity. The ADC_w map shown in Figure 2D was generated by fitting the signal intensity of each pixel to Eq. (1), as described in Materials and Methods. The structural details seen in Figure 2A to C are also observed in the ADC_w map. However, the ADC_w map is a quantitative representation of absolute values wherein the higher D values are bright, and the DWI in Figure 2A to C show only relative values, with higher D values being dark due to signal attenuation.

Effect of Paclitaxel on the Distribution of ADC_w Values of Tumors

Twenty-four MCF7/S and MCF7/D40 tumors (6 treated and 6 controls of each type) were analyzed by tumor volume and DWI for 7 days after commencement of Paclitaxel CTx. As shown in Figure 3C and D, Paclitaxel arrested growth in all MCF7/S tumors and had no effect on the tumors from MCF7/D40 cells. After DWI examinations, the data were fit on a pixel-by-pixel basis, and ADC_w maps were generated for each tumor. These data were expressed as a histogram of pixel incidence versus ADC_w. As the tumors were remarkably homogeneous within a group, the ADC distribution was averaged for each group of tumors.

Figure 3A and B show histograms of ADC_w values in treated versus untreated tumors for both cell types 48 hours after the start of Paclitaxel CTx. In MCF7/S tumors, the ADC_w distribution in untreated tumors was $0.5 \sim 0.7 \times 10^{-9}$ m^2/s, which was not notably different from the range observed in tumors before treatment. However, in the treated tumors, the ADC_w values were 0.7 to 1.5×10^{-9} m^2/s. In contrast, both treated and untreated MCF7/D40 tumors exhibited ADC_w values similar to those observed in tumors before treatment. Note also that these changes in the ADC_w were apparent 2 days after commencement of CTx. Although there are observable differences in tumor volumes between treated and controls by day 2 (Figure 3C and D), these are not significant.

Discussion

Mechanism of ADC Changes

The mechanism underlying the change in ADC_w after chemotherapy is unknown. However, data from other systems (e.g., stroke) indicate a direct relationship between ADC_w and the extracellular volume fraction. If this mechanism also dominates the ADC_w values observed in tumors, then the higher values observed after CTx of the drug-sensitive tumors would be consistent with a decrease in the intracellular water after Paclitaxel-induced apoptosis. Paclitaxel is known to kill tumor cells via apoptosis [23–26]. A hallmark of apoptosis is a reduction of cell volume via blebbing. Benson et al. have shown that the decreases in cell volume during apoptosis are biphasic, with an early rapid phase that is reversible and a slower, irreversible phase associated with chromosome condensation and DNA hydrolysis [27]. A recent study by Hakumaki et al. (1998) showed a 219% increase in the ADC_w of water in viral thymidine kinase–containing tumors induced to apoptosis with ganciclovir [28]. In this system the relative fraction of extracellular water grew from 87% to 94% in response to CTx. The authors concluded that the measured nuclear magnetic resonance parameters could describe the biophysical signatures for apoptotic cell death.

Mechanism of Paclitaxel CTx

Previous studies investigating the response of ADC_w to CTx used exclusively cytotoxic drugs. It would be of interest to know if these changes also occur in modern cytostatic drugs. Paclitaxel has both cytostatic and cytotoxic properties. Clinically, Paclitaxel produces partial cytostasis (approximately 30% maximum) and apoptosis (maximum apoptotic index of 3.3% to 29%) in human breast tumors [23]. In SKOV3 ovarian carcinoma cells treated with Paclitaxel, the first cellular effect observed with continuous exposure to 50 ng/mL paclitaxel (ID50) was mitotic arrest, followed by DNA fragmentation, first detected at 24 hours and peaking at 48 hours. In this particular study, apoptosis was correlated with an induction and activation of the c-Mos gene product. [24]. Similar results were obtained in 3-dimensional histocultures of ovarian tumors surgically removed from patients ($n = 17$). Paclitaxel was shown to produce a partial inhibition of DNA precursor incorporation in about 40% of tumors and to induce apoptosis in about 90% of tumors, with a maximum apoptotic index of 15% [25]. Finally, in an extensive study of 6 differents cell lines, including bladder RT4, breast MCF7, pharynx FaDu, ovarian SKOV3, and prostate PC3 and DU145, Paclitaxel treatment for as brief a period as 3 hours was sufficient to induce apoptosis, which occurred with a lag time of about 24 hours. The intracellular and extracellular concentrations of the drug reached an equilibrium at approximately 5 hours after the beginning of treatment [26]. Thus, our results are consistent with the triggering of apoptosis by Paclitaxel in MCF7/S tumors, which induces a larger extracellular space, shifting the ADC_w to higher values.

ADC_w and MDR

An important aspect of the current study is that Paclitaxel-induced effects were not observed in MCF7/D40 cells, a P-gp-positive cell line. P-gp is an ATP-dependent drug efflux pump that increases drug efflux when overexpressed. P-gp expression renders cells cross-resistant to a wide variety of drugs [29,30]. The defective accumulation of Paclitaxel in P-gp overexpressing breast cancer cell lines was demonstrated with ^{14}C-Paclitaxel [7]. In another study Mechetner et al. showed a strong correlation between the degree of P-gp expression and *in vitro* resistance to Paclitaxel and doxorubicin in MCF-7/D40 cells [8]. Accordingly,

we did not see any effect of Paclitaxel treatment on the MCF7/D40 tumors in this study. It is noteworthy that Paclitaxel has also been shown to have antiangiogenic activity [31,32]. Presumably this could also have an effect on ADC values as it would decrease the perfusion of the tumor to induce hypoxia and subsequently trigger aptopotic cell death as well. This does not seems to be the case, however, because resistant and sensitive cells should have the same vascular beds, and yet there were distinct responses of ADC_w to CTx. The fact we do not see any Paclitaxel activity in MCF7/D40 tumors indicates that antiangiogenic effects are negligible at this stage of treatment (2 days after a 28 mg/kg Paclitaxel intraperitoneal injection).

Conclusions

The results presented herein show that DWI can identify CTx response and discriminate between sensitive and resistant breast carcinoma tumors at an early stage of chemotherapy, i.e., before frank changes in tumor volume are significant. Moreover, DWI can give a unique insight into the spatial distribution of CTx effects within a tumor over the course of treatment. This method can be easily adapted to the clinic and has the potential to become a noninvasive tool to evaluate the efficacy of CTx treatment in humans.

References

[1] Clemons M, Leahy M, Valle J, Jayson G, Ranson M, and Howell A (1997). Review of recent trials of chemotherapy for advanced breast cancer: The taxanes. *Eur J Cancer* **33**, 2183–2193.

[2] Chenevert TL, and Ross BD (1995). Diffusion, T1 and T2 as chemotherapeutic response predictors of experimental brain tumors. *Proc Int Soc Magn Reson Med* **2**, p. 924.

[3] Chenevert TL, McKeever PE, and Ross BD (1997). Monitoring early response of experimental brain tumors to therapy using diffusion magnetic resonance imaging. *Clin Cancer Res* **3**, 1457–1466.

[4] Zhao M, Pipe JG, Bonnett J, and Evelhoch JL (1996). Early detection of treatment response by diffusion-weighted 1H-NMR spectroscopy in a murine tumour *in vivo*. *Br J Cancer* **73**, 61–64.

[5] Zhao M, and Evelhoch JL (1996). Detection of response to 5-fluorouracil by diffusion-weighted 1H NMR spectroscopy in murine tumors *in vivo*. *Proc Int Soc Magn Reson Med* **2**, p. 1118.

[6] Rowinsky EK (1997). Paclitaxel pharmacology and other tumor types. *Semin Oncol* **24** [suppl 19], S19-1-S19-12.

[7] van Ark-Otte J, Samelis G, Rubio G, Lopez Saez JB, Pinedo HM, and Giaccone G (1998). Effects of tubulin-inhibiting agents in human lung and breast cancer cell lines with different multidrug resistance phenotypes. *Oncol Rep* **5**, 249–255.

[8] Mechetner E, Kyshtoobayeva A, Zonis S, Kim H, Stroup R, Garcia R, Parker RJ, and Fruehauf JP (1998). Levels of multidrug resistance (MDR1) P-glycoprotein expression by human breast cancer correlate with *in vitro* resistance to paclitaxel and doxorubicin. *Clin Cancer Res* **4**, 389–398.

[9] Moseley ME, Kucharczyk J, Mintorovitch J, Cohen Y, Kurhanewicz J, Derugin N, Asgari H, and Norman D (1990). Diffusion-weighted MR imaging of acute stroke: Correlation with T2-weighted and magnetic susceptibility-enhanced MR imaging in cats. *AJNR: Am J Neuroradiol* **11**, 423–429.

[10] Moseley ME, Cohen Y, Mintorovitch J, Chileuitt L, Shimizu H, Kucharczyk J, Wendland MF, and Weinstein PR (1990). Early detection of regional cerebral ischemia in cats: Comparison of diffusion- and T2-weighted MRI and spectroscopy. *Magn Reson Med* **14**, 330–346.

[11] Fischer M, Bockhorst K, Hoehn-Berlage M, Schmitz B, and Hossmann KA (1995). Imaging of the apparent diffusion coefficient for the evaluation of cerebral metabolic recovery after cardiac arrest. *Magn Reson Imaging* **13**, 781–790.

[12] Latour LL, Svoboda K, Mitra P, and Sotak CH (1994). Time-dependent diffusion of water in a biological model system. *Proc Natl Acad Sci USA* **91**, 1229–1233.

[13] Szafer A, Zhong J, and Gore JC (1995). Theoretical model for water diffusion in tissues. *Magn Reson Med* **33**, 697–712.

[14] van Gelderen P, de Vleeschouwer MH, DesPres D, Pekar J, van Zijl PC, and Moonen CT (1994). Water diffusion and acute stroke. *Magn Reson Med* **31**, 154–163.

[15] Warach S, Gaa J, Siewert B, Wielopolski P, and Edelman RR (1995). Acute human stroke studied by whole brain echo planar diffusion-weighted magnetic resonance imaging. *Ann Neurol* **37**, 231–241.

[16] Galons JP, Trouard T, Gmitro AF, and Lien YH (1996). Hemodialysis increases apparent diffusion coefficient of brain water in nephrectomized rats measured by isotropic diffusion-weighted magnetic resonance imaging. *J Clin Invest* **98**, 750–755.

[17] Ross BD, Chenevert TL, Kim B, and Ben-Yoseph O (1994). Magnetic Resonance Imaging and Spectroscopy: Application to Experimental Neuro-Oncology. *Q Magn Reson Biol Med* **1**, 85–102.

[18] Taylor CW, Dalton WS, Parrish PR, Gleason MC, Bellamy WT, Thompson FH, Roe DJ, and Trent JM (1991). Different mechanisms of decreased drug accumulation in doxorubicin and mitoxantrone resistant variants of the MCF7 human breast cancer cell line. *Br J Cancer* **63**, 923–929.

[19] Paine-Murrieta GD, Taylor CW, Curtis RA, Lopez MH, Dorr RT, Johnson CS, Funk CY, Thompson F, and Hersh EM (1997). Human tumor models in the severe combined immune deficient (scid) mouse. *Cancer Chemother Pharmacol* **40**, 209–214.

[20] Taetle R, Rosen F, Abramson I, Venditti J, and Howell S (1987). Use of nude mouse xenografts as preclinical drug screens: *in vivo* activity of established chemotherapeutic agents against melanoma and ovarian carcinoma xenografts. *Cancer Treat Rep* **71**, 297–304.

[21] Altbach MI, Mattingly MA, Brown MF, and Gmitro AF (1991) Magnetic resonance imaging of lipid deposits in human atheroma via a stimulated-echo diffusion-weighted technique. *Magn Reson Med* **20**, 319–324.

[22] Basser PJ, and Pierpaoli C (1996). Microstructural and physiological features of tissues elucidated by quantitative-diffusion-tensor MRI. *J Magn Reson B* **111**, 209–219.

[23] Gan Y, Wientjes MG, Lu J, and Au JL (1998). Cytostatic and apoptotic effects of paclitaxel in human breast tumors. *Cancer Chemother & Pharmacol* **42**, 177–182.

[24] Ling YH, Yang Y, Tornos C, Singh B, and Perez-Soler R (1998). Paclitaxel-induced apoptosis is associated with expression and activation of c-Mos gene product in human ovarian carcinoma SKOV3 cells. *Cancer Res* **58**, 3633–3640.

[25] Millenbaugh NJ, Gan Y, and Au JL (1998). Cytostatic and apoptotic effects of paclitaxel in human ovarian tumors. *Pharm Res* **15**, 122–127.

[26] Au JL, Li D, Gan Y, Gao X, Johnson AL, Johnston J, Millenbaugh NJ, Jang SH, Kuh HJ, Chen CT, and Wientjes MG (1998). Pharmacodynamics of immediate and delayed effects of paclitaxel: Role of slow apoptosis and intracellular drug retention. *Cancer Res* **58**, 2141–2148.

[27] Benson RS, Heer S, Dive C, and Watson AJ (1996). Characterisation of cell volume loss in CEM-C7A cells during dexamethasone-induced apoptosis. *Am J Physiol* **270**(4pt1), C1190–C1230.

[28] Hakumaki JM, Poptani H, Puumalainen AM, Loimas S, Paljarvi LA, Yla-Herttuala S, and Kauppinen RA (1998). Quantitative ^{1}H nuclear magnetic resonance diffusion spectroscopy of BT4C rat glioma during thymidine kinase-mediated gene therapy *in vivo*: Identification of apoptotic response. *Cancer Res* **58**, 3791–3799.

[29] Simon SM, and Schindler M (1994). Cell biological mechanisms of multidrug resistance in tumors. *Proc Natl Acad Sci USA* **91**, 3497–3504.

[30] Nielsen D, and Skovsgaard T (1992). P-glycoprotein as multidrug transporter: A critical review of current multidrug resistant cell lines. *Biochim Biophys Acta* **1139**, 169–183.

[31] Klauber N, Parangi S, Flynn E, Hamel E, and D'Amato RJ (1997). Inhibition of angiogenesis and breast cancer in mice by the microtubule inhibitors 2-methoxyestradiol and paclitaxel. *Cancer Res* **57**, 81–86.

[32] Belotti D, Vergani V, Drudis T, Borsotti P, Pitelli MR, Viale G, Giavazzi R, and Taraboletti G (1996). The microtubule-affecting drug paclitaxel has antigiogenic activity. *Clin Cancer Res* **2**, 1843–1849.